Innovative: International Multi-disciplinary Journal of Applied Technology
(ISSN 2995-486X) VOLUME 04 ISSUE 01, 2026

Mathematical Modelling and Hydrodynamic Assessment of a Frame–Elastic Barrier for Dissipating the Energy of Climate Change-Induced Debris Flows and Floods in Mountainous and Foothill Regions

PhD, Associate professor G.M. Gulomova
Senior Lecturer M.B. Barotov
(Tashkent State Technical University named after Islam Karimov)

Abstract:

This article presents the hydrodynamic basis, the mathematical model, and the computational algorithm of a flexible frame-net barrier structure that dissipates, through elastic deformation, the dynamic impact of debris flows and floods in the mountainous and foothill regions of Uzbekistan (using the Bostonliq district as a case study) under climate change conditions. In the study, analytical equations were developed to determine the dependence of the erosion coefficient of mountain slopes on time, the maximum peak discharge of the flow, and the specific impact pressure exerted on the structure by a two-phase debris mass. Laboratory experiments conducted on the basis of Froude similarity criteria proved that the elastic structure is capable of dissipating up to 63.8% of the kinetic energy, which provides an efficiency 25-30% higher than that of conventional rigid dams. Based on the analysis of full-scale field trials of the structure (involving a debris mass of 115 m³ and a 1.15-tonne boulder), it was established that the impact pressure is distributed parabolically along the height of the structure and that the critical point is located within the lower one third of the height. A unified mathematical model integrating the hydrological, hydrodynamic, and energy blocks, together with an iterative computational algorithm that jointly verifies the strength and efficiency conditions, was proposed. The results obtained serve as a practical engineering tool for the scientifically grounded design of such structures in mountain watersheds under climate change conditions.

Keywords: *debris flow and flood; elastic frame barrier; hydrodynamic impact pressure; energy dissipation; mathematical modeling; iterative algorithm; climate change; Bostonliq district*

Introduction

Over the past decade, global climate change has significantly altered the extreme indicators of hydrometeorological processes in the mountainous and foothill regions of the Republic of Uzbekistan. The rise in the mean annual air temperature and the anomalous distribution of the intensity of atmospheric precipitation have accelerated ablation processes in mountain systems and are disrupting the stability of moraine lakes in the upper watersheds. As a result, the probability of the formation of debris flows and floods rich in solid sediment and possessing high kinetic energy is steadily increasing.

Modeled weather data have a resolution of approximately 30 km and may not reproduce all local weather effects such as thunderstorms, local winds, or tornadoes, nor the local variations that occur in urban, mountainous, or coastal areas. [5]

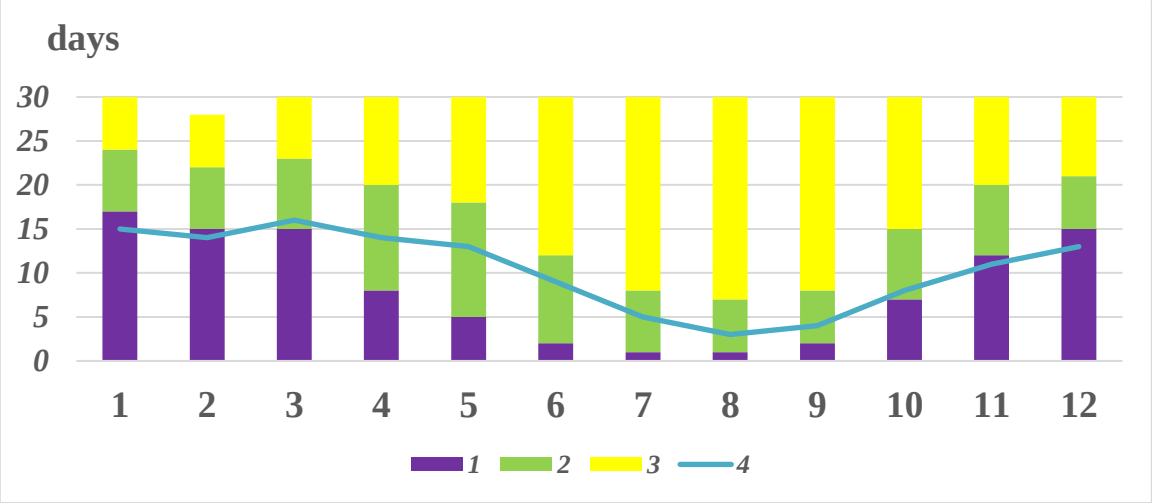

Figure 1. Graph of the variation of cloud cover, sunshine, and precipitation days at the Chimyon, Chorvoq, Ugom, and Chotqol meteorological stations: 1 - sunshine; 2 - partly cloudy; 3- fully cloudy; 4 - days with precipitation.

The maximum mean daily temperature (dark red line) shows the maximum mean temperature for individual days of the month for Chimyon. Similarly, the minimum mean daily temperature (dark blue line) shows the minimum mean temperature; the warm days and cold nights (dotted red and blue lines) show the mean temperature of the hottest day and the coldest night of each month over a 30-year period.

Figure 2. Cumulative diagram of the variation of maximum temperatures for the Chimyon,

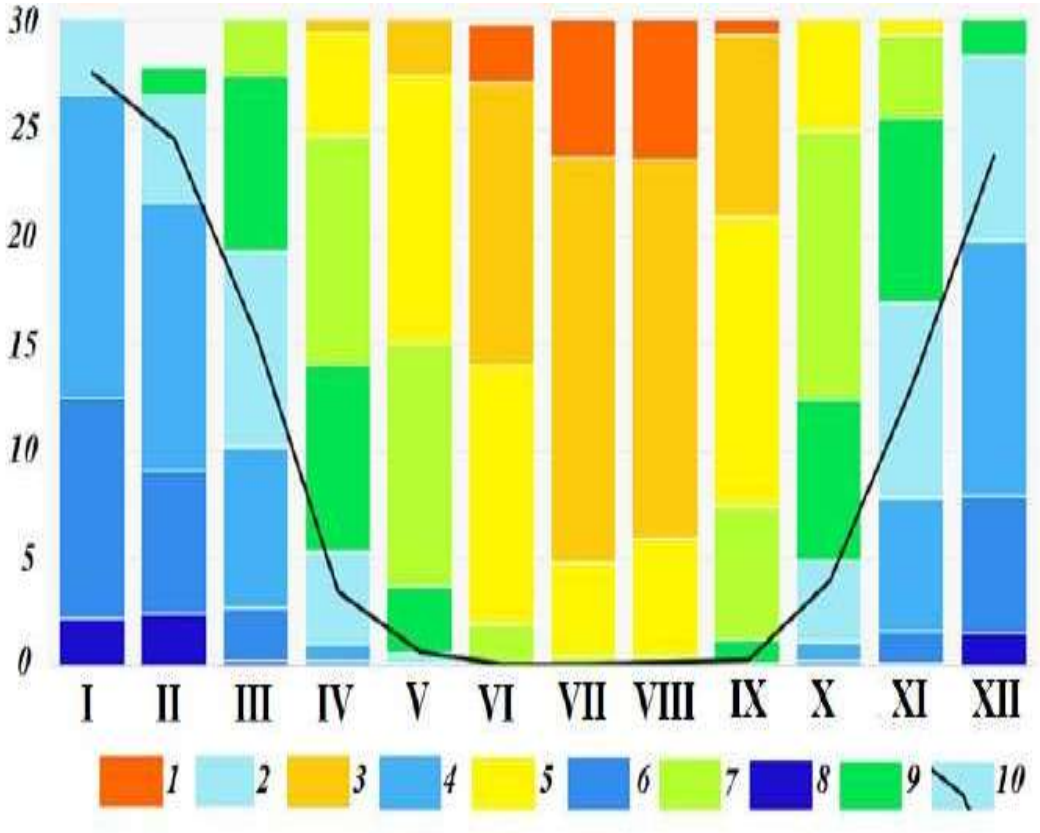

Chorvoq, Ugom, and Chotqol weather stations: 1 - >30; 2 - >5; 3 - >25; 4 - ≥0; 5 - <20; 6 - <0; 7 - >15; 8 - <5; 9 - 10; 10 - cold days, by month of the year

Table 1

Table of the mean days of the year by cloud cover, sunshine, and precipitation

Months	Jan.	Feb.	Mar.	Apr.	May	Jun.	Jul.	Aug.	Sep.	Oct.	Nov.	Dec.
Sunny	7,4	6,1	7,1	9	12,4	17,6	23,2	24,7	22,4	15,7	9,7	9,4
Partly cloudy	6,6	6,8	8,8	12,1	13,8	10,5	7	5,5	5,6	8,4	7,8	6
Cloudy	17	15,4	15,1	8,9	4,8	1,8	0,9	0,8	1,9	6,8	12,5	15,6
Days with precipitation	15	14,2	16,6	14,5	13,5	9,3	4,5	2,4	3,1	7,8	11,1	13,8

The graph shows the number of sunny, partly cloudy, and foggy days, as well as the days with precipitation (Figure 2 and Table 1). Days on which the cloud layer does not exceed 20% are considered sunny; a cloud layer of 20-80% is considered partly cloudy, and more than 80% is considered fully cloudy. When planning a holiday, one becomes aware of the mean temperature and

also pays attention to the hottest days and, in the cold season, to the coldest days (Figure 1 and Table 2).

The diagram of maximum temperatures in Chimyon shows the number of days in each month on which a particular temperature was reached (Figure 3, Table 2). In Dubai, one of the hottest cities on Earth, the temperature in July hardly falls below 40 ^{0}C. One may also examine a diagram of the cold winters in Moscow, which shows that on several days of that month the maximum temperature barely reaches -10 ^{0}C.

The precipitation diagram for Chimyon shows on how many days per month a particular amount of precipitation falls. For example, in regions with a tropical or monsoon climate, the forecast of rainfall may be underestimated.

Table 2

Table of mean daily temperature by month of the year

	Jan.	Feb.	Mar.	Apr.	May	Jun.	Jul.	Aug.	Sep.	Oct.	Nov.	Dec.
>30 *ºC*	0	0	0	0	0	2,7	7,1	7,2	0,6	0	0	0
>25 *ºC*	0	0	0	0,6	3,5	13,2	18,9	17,7	8,5	0,5	0	0
>20 *ºC*	0	0	0	4,8	12,5	12,1	4,4	5,5	13,5	5,5	0,6	0
->15 *ºC*	0	0	3,2	10,7	11,3	1,9	0,4	0,4	6,2	12,5	3,9	0,2
>10 *ºC*	0	1,3	8,2	8,7	3,1	0	0	0	1,1	7,5	8,6	2,3
>5 *ºC*	3,7	5	9,1	4,3	0,5	0	0	0	0,1	3,8	9,1	8,6
≥ *0 ºC*	14,1	12,5	7,2	0,8	0,1	0	0	0	0	0,9	6,2	11,9
<0 ºC	10,3	6,7	2,5	0,2	0	0	0	0	0	0,2	1,5	6,4
<-5 *ºC*	2,2	2,4	0,2	0	0	0	0	0	0	0	0,1	1,5
Cold days	27,6	24,5	15,4	3,4	0,6	0	0	0,1	0,2	3,9	13	23,7

The diagram for Chimyon likewise makes it possible to estimate the wind speed for each month at a particular value. Long, strong winds from December to April and calm air currents from June to October are of interest. The wind-speed diagram for Chimyon shows how many hours per year the wind blows from a particular direction. According, the wind blows from the south-west (SW) towards the north-east (NE).

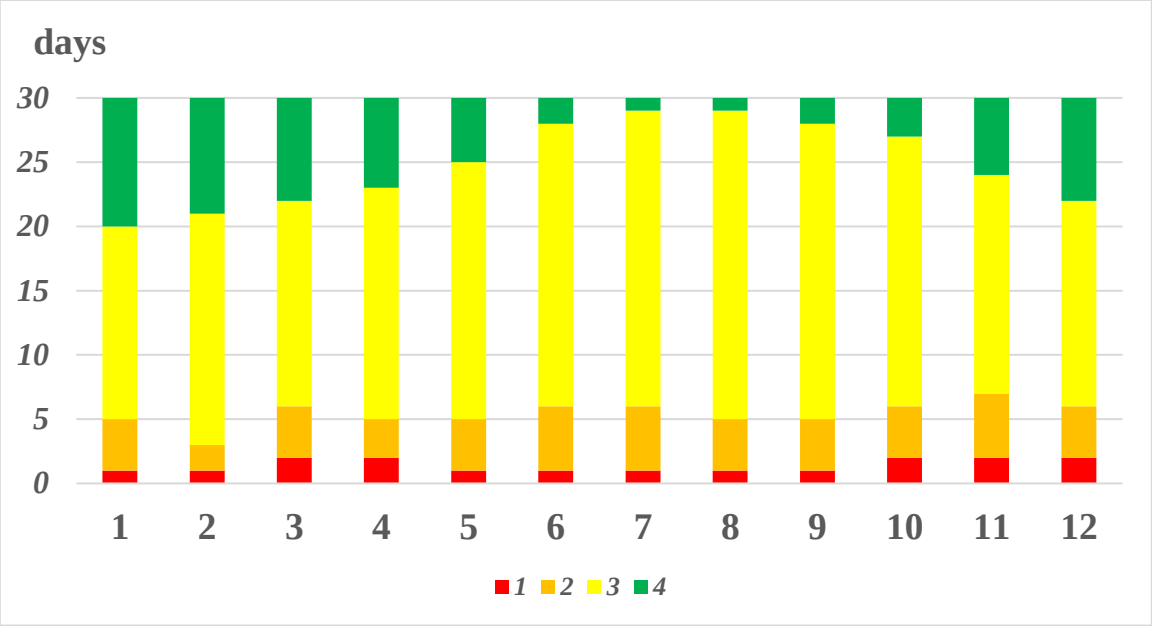

Figure 3. Cumulative diagram of the variation of wind speed at the Chimyon, Chorvoq, Ugom, and Chotqol meteorological stations (m/s): 1 - 0; 2 - 12; 3 - 19; 4 - 28;

The Bostonliq district of the Tashkent region - an area encompassing the Chimgonsoy, Pskom, Ugom, and Chotqol basins of the Western Tien Shan mountain system - is regarded as the model area in which these processes manifest themselves with the highest intensity. [11] The rigid hydraulic structures traditionally employed in the region (monolithic concrete dams, walls) are not demonstrating the expected effect in withstanding the high dynamic impact of debris flows and the mechanically destructive action of solid fractions (large rock blocks, tree trunks), because such structures are designed as non-deformable rigid systems and dissipate the impact energy solely through reflection.

Although flexible (elastic) barrier structures based on energy dissipation have been developed in international practice by researchers such as G.V. Gavardashvili and B. McArdell, the existing solutions are adapted mainly to the conditions of the Alpine and Caucasian mountain systems. A hydrodynamically substantiated and field-validated comprehensive mathematical model that takes into account the high seismic activity, the predominance of loess-like rocks, and the specific hydrological regime characteristic of Central Asia - and of the Western Tien Shan region of Uzbekistan in particular - has so far not been sufficiently developed in the scientific literature. It is precisely this methodological gap that determines the scientific relevance of the present study. [10]

The aim of the study is to develop the hydrodynamic principles of a frame-elastic barrier structure that dissipates the dynamic impact of debris-flow and flood currents through elastic deformation, to validate its effectiveness experimentally under laboratory and real field conditions, and to create a unified mathematical model and an iterative computational algorithm that jointly satisfy the strength and efficiency conditions. The scientific novelty of the study consists in the following: (i) the law of the parabolic distribution of the impact pressure along the height of the structure was determined experimentally under field conditions for the first time; a unified iterative algorithm integrating the hydrological, hydrodynamic, and energy blocks was proposed; the results were validated on a full-scale engineering structure, which ensures a complete scientific cycle from the theoretical model to practical implementation. [12]

Object and area of the study. The basins of the Chimgonsoy, Oqsoqotasoy, Pskom, Ugom, and Chotqol rivers of the Bostonliq district of the Tashkent region were selected as the object of the study. This area is located in the part of the Western Tien Shan mountain system that consists of a junction of complex tectonic blocks and is characterized by strongly dissected relief, high slope angles, and seismic activity (7-9 points). Because channel activity and the proportion of erosion are high in the small hydrographic basins (Chimgonsoy and Oqsoqotasoy), the erosion coefficient increases more rapidly over time, which turns these streams into a priority zone of the first order for the installation of elastic barriers. This combination of characteristics defines the area as a typical model site for testing the hydrodynamic efficiency of the frame-elastic barrier structure.

Engineering and structural configuration of the structure. Taking into account the narrow and deep channel relief of mountain rivers and the powerful impact impulse of the debris-flow front, the load-bearing base of the structure was designed in the form of a system of bearing metal frames made of high-strength steel components. The structure was assembled as a unified spatial system receiving permanent and temporary dynamic loads: metal ropes (cables) with a high elasticity coefficient and square openings measuring 0.20×0.20 m² are suspended from stepped (cascade) tiered metal frames, which places the structure in the category of open (perforated) filtering dams. Individual point foundation blocks were used for each supporting frame; these were constructed from a W8 waterproof concrete mixture belonging to a high engineering class and are designed to withstand seismic vibrations and displacing hydrodynamic stresses. The foundation section is fully waterproofed against the effects of aggressive groundwater in the rock mass and of subsurface filtration.

Hydrological and hydrodynamic mathematical model. The erosion coefficient (E) of mountain slopes with respect to the time function was determined by means of the following refined equation:

$$E = 0.58 + 1.40 \cdot (F_1/F_0) \cdot (t/T)^{0.21}$$

where F_1 is the eroded active area within the basin (km²); F_0 is the total area of the basin (km²); t is the computational time interval (years); T is the multi-year observation period.

The maximum peak discharge of the flow (Qmax) at various supply reserves was calculated by means of the following empirical relationship:

$$Q_{max} = A \cdot (34 + 400 \cdot i) \cdot F_0^{0.61} \quad [m^3/s]$$

where is the mean longitudinal slope of the channel (m/m); A is the discharge coefficient depending on the level of exceedance probability (P, %). In order to ensure high reliability for civil-protection structures, A = 1.0 was adopted (1% exceedance probability, once in 100 years).

The specific hydrodynamic impact pressure (P_1) exerted by the two-phase debris flow on the body of the structure was determined by means of the fundamental equation:

$$P_1 = (\gamma \cdot w \cdot V^2 / g) \cdot \sin\psi \cdot f(m) \quad [N/m^2]$$

where γ is the bulk weight of the flow mass (14000–18000 N/m³); w is the effective cross-sectional area perpendicular to the barrier; V is the linear velocity of the flow; g is the acceleration of free fall; ψ is the internal friction (impact) coefficient, $\psi = \tan^2(45° - \varphi/2)$; f(m) is the functional coefficient expressing the state of the flow layer; φ is the angle of internal friction of the solid fractions.

Laboratory experimental methodology. With the aim of studying in depth the dynamics of flow motion, the screening (sorting) of solid rock fractions, and the indicators of kinetic-energy dissipation, experimental modeling was carried out in a special hydraulic laboratory flume

(longitudinal bed slope i = 0.01÷0.06). In order to ensure geometric and hydrodynamic similarity, the condition of the mutual equality of the Froude criterion was applied:

$$V^2_{nat} / (2g \cdot H_{nat}) = V^2_{mod} / (2g \cdot H_{mod})$$

In addition to this condition, geometric and slope proportionality ($i_{nat} = i_{mod}$), the drift-suspension equilibrium of the phases, and the correspondence of the Chézy resistance coefficient were ensured. The overall geometric dimensions of the structure were adopted as follows: transverse width - 1.0 m, longitudinal length – 1.50 m, maximum structural height - 0.50 m. The model was formed of three tiered triangular prisms of increasing height arranged consecutively along the direction of the hydraulic flow (Figure 4); the base length of each prism is 0.50 m, and the upward increase in slope provided the "springboard effect", which directs the front of the oncoming wave into the vertical component.

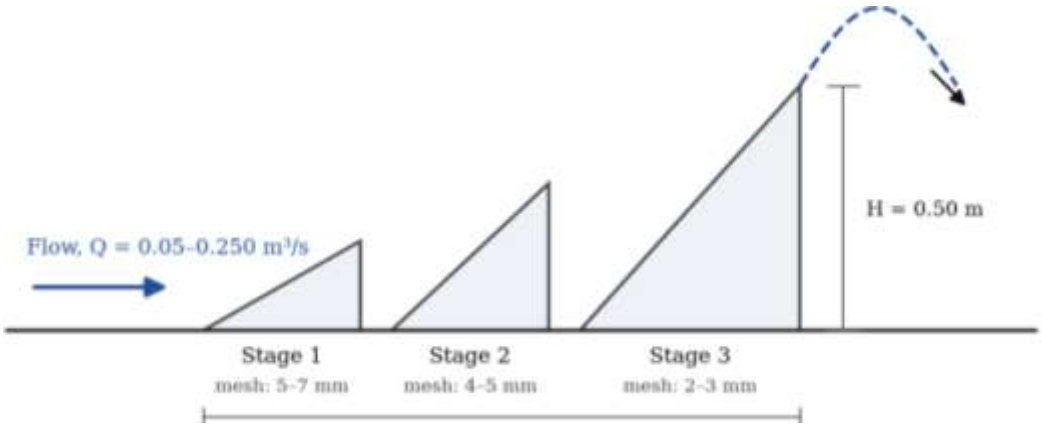

Figure 4. Longitudinal section of the laboratory cascade elastic barrier model and geometric parameters of the net tiers

Three types of open-mesh symmetric nets were installed on the surfaces of the prisms for the mechanical sorting of solid fractions and were subjected to testing: an opening size of 5÷7 mm on the first tier, 4÷5 mm on the second tier, and 2÷3 mm on the third tier. The experiments were conducted within a discharge range of Q = 0.05-0.250 m³/s.

Theory of hydraulic resistance and energy loss. In the quantitative assessment of the hydraulic efficiency of the cascade elastic barrier, its local resistance coefficient (ζ) plays a leading role. On the basis of the generalization of the updated wide-flume (B = 1.0 m) laboratory data, this coefficient was determined by means of the following dimensionless criterial equation:

$$\zeta = (1/\varphi^2 - 1) \cdot ((1 - \Omega)/\Omega)^{1.75}$$

where φ = 0.85–0.91 is the velocity coefficient of the flow passing through the openings of the elastic barrier; Ω is the perforation coefficient of the barrier, $\Omega = \omega_{openings} / \omega_{total}$. The hydraulic jump and energy loss arising as a result of the springboard effect at the foot of the cascade were calculated using the modified Bernoulli equation:

$$\Delta E_{kin} = \zeta \cdot V1^2/(2g) + (H_1 + p_1/\gamma_s) - (H_2 + p_2/\gamma s)$$

where p_1 and p_2 are the hydrodynamic pressure values before and after the barrier (Pa); γs is the mean mixture density of the flow (14000÷18000 N/m³). The share of dissipated kinetic energy (the efficiency coefficient, η) was determined by means of the following ratio:

$$\eta = (E_{kir} - E_{chiq}) / E_{kir} \cdot 100\%$$

Methodology of separating the two-phase flow into fractions and of field testing. The frame-elastic barrier structure based on the laboratory results was installed at full scale in a gully of the Bostonliq district with a naturally high debris-flow hazard. During the field monitoring, the volume of the debris mass acting on the structure, the parameters of the retained solid fractions, the pressure distribution along the height of the structure, and the values of the channel slope before and after the installation of the structure were recorded. The two-stage decision algorithm expressing the mechanism of the dynamic sorting of the solid and liquid phases within the flow is presented in Figure 5: at the first stage, the fraction size (d) is compared with a threshold value (d = 0.20 m) - fractions larger than this are retained by the metal net, while smaller ones are filtered through freely; at the second stage, the calculated dynamic pressure (P_{dyn}) is compared with the limiting pressure (P_{lim}), and the elastic or linear operating regime of the structure is selected.

Mathematical model and iterative computational algorithm. Whereas the hydrodynamic principles of the frame-elastic net barrier presented above (the erosion coefficient E(t), the maximum peak discharge Qmax, the dynamic impact pressure P_1, and the energy dissipation coefficient η) were presented together with the results of laboratory modeling, the field trials of this structure under real mountain conditions (in the basins of the Bostonliq district), including the successful restraint of a debris mass of 115 m³ in volume and of a boulder weighing 1.15 tonnes, were described. The aim of the present section is to generalize, within a unified mathematical model, the hydrological, hydrodynamic, and energy processes analyzed separately in the two preceding sections, and to develop an iterative computational algorithm that predicts the dynamic state of the structure.

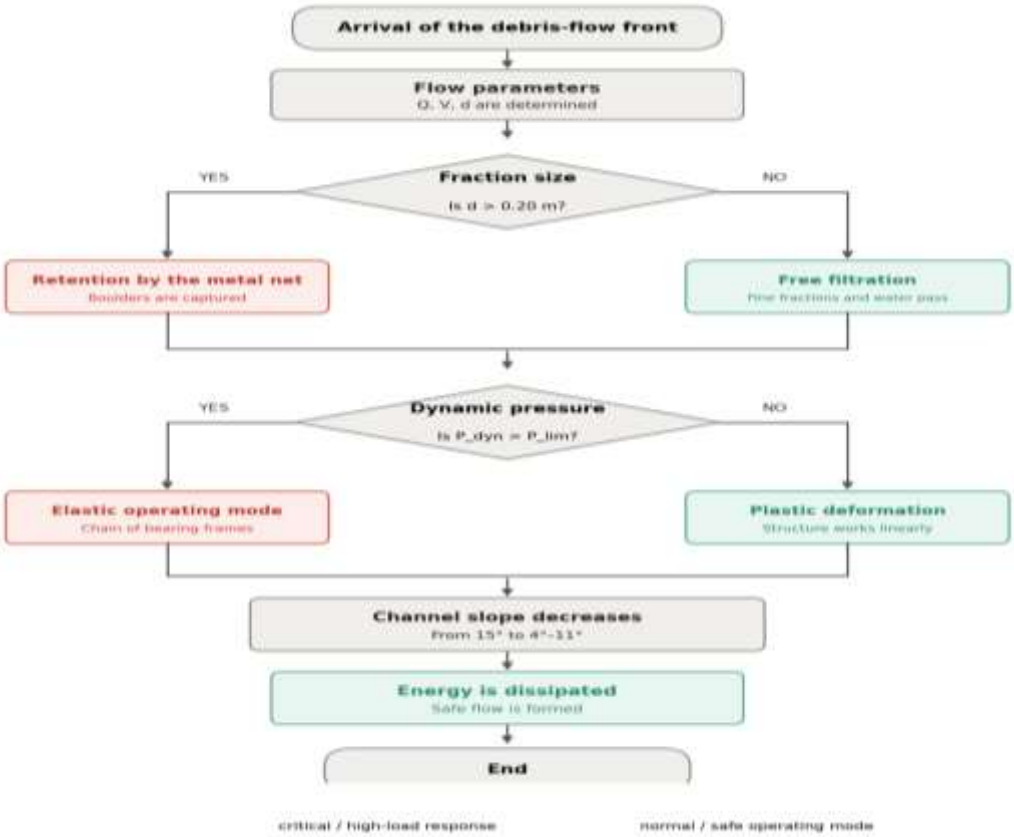

Figure 5. Block diagram of the algorithm for separating the debris flow into fractions and controlling the dynamic pressure

The proposed model integrates three interrelated blocks - the hydrological block (determination of the flow discharge), the hydrodynamic block (calculation of the impact pressure and of its distribution along the height), and the energy block (assessment of the dissipation of kinetic energy and of the reduction in the level of damage). The novelty of the model lies in the fact that, unlike conventional rigid dams, it takes into account the parabolic distribution of the impact force along the height of the structure and the step-by-step dissipation of energy through elastic deformation.

Mathematical formulation of the problem and principal assumptions. The two-phase (water + solid phase) debris flow acting on the frame-elastic barrier is regarded as a non-stationary turbulent flow. The following principal assumptions were adopted in constructing the model:

the mean bulk weight of the flow mass γ is assumed to be constant within the computational interval (14000-18000 N/m³);

the sorting of solid fractions at the net openings (0.20×0.20 m) is taken into account by means of a semi-empirical filtration coefficient;

the structure operates as a unified spatial elastic system and distributes the impact impulse to the slope anchor cables;

the hydraulic jump and energy dissipation occur consecutively along the cascade tiers.

The ultimate aim of the calculation is to maximize the following objective function, namely the share of kinetic energy dissipated by the structure (the efficiency criterion):

$$\eta = (E_{kir} - E_{chiq}) / E_{kir} \cdot 100\% \rightarrow max, \quad shart: \ P_{max} \le [P_{dop}]$$

where E_{in} is the kinetic energy of the flow at the entry to the barrier; E_{out} is the residual energy after passage through the barrier; $[P_{adm}]$ is the permissible (design) impact pressure of the frame material.

Hydrological block - determination of the flow discharge. At the first stage of the model, the erosion state of the basin and the maximum peak discharge are determined on the basis of the substantiated formulas. The erosion coefficient of the mountain slopes as a function of time:

$$E = 0.58 + 1.40 \cdot (F_1/F_0) \cdot (t/T)^{0.21}$$

The quantity of the solid phase estimated by means of the erosion coefficient determines the bulk weight γ of the flow. Having adopted the discharge coefficient A corresponding to the selected level of exceedance probability (P, %), the maximum peak discharge is calculated as follows:

$$Q_{max} = A \cdot (34 + 400 \cdot i) \cdot F_0^{0.61} \quad [m^3/s]$$

In order to ensure high reliability for civil-protection structures, A = 1.0 is adopted at a 1% exceedance probability. The mean velocity V of the flow is determined by the Chézy formula or by the continuity equation $V = Q_{max} / w$ and serves as an input parameter for the next block.

Hydrodynamic block - impact pressure and distribution along the height. On the basis of the determined velocity and flow density, the specific dynamic impact pressure acting on the surface of the barrier is calculated by means of the fundamental equation:

$$P_1 = (\gamma \cdot w \cdot V^2 / g) \cdot \sin\psi \cdot f(m) \quad [N/m^2]$$

The auxiliary coefficients are determined as follows:

$$\psi = \tan^2(45° - \varphi/2); \quad \alpha = (1 - h_0) \cdot \psi$$

where φ is the angle of internal friction of the solid fractions; h_0 is the equivalent bonding depth of the flow; f(m) is the functional coefficient expressing the state of the flow layer in the area of the foundation of the structure.

The principal scientific novelty of the present study is the mathematical description of the fact that the impact pressure is distributed along the height (z) of the structure not uniformly, but according to a parabolic law. According to the recorded field observations, when the level of the rock material accumulated in the net reaches 1.0 m and a 1.15 t boulder strikes the structure, the maximum pressure is located within the lower one third of the height (the critical point $z^* = H_{t/3}$). The distribution of the pressure along the height is expressed by means of the following parabolic model:

$$P(z) = P_{max} \cdot [\, 1 - ((z - z^*) / z^*)^2 \,], \quad 0 \le z \le H_t$$

Here $P_{max} = P_1$ is the maximum pressure value (at the critical point), and H_t is the design height of the structure together with the accumulated rock material. This profile makes it possible, with the aid of the bearing frames and the elastic anchor cables, to distribute the stress at the critical point stationarily to the slopes, and it eliminates the risk of overturning of the foundation blocks.

Energy Block - Dissipation of Kinetic Energy. In order to assess quantitatively the hydraulic efficiency of the barrier, the local resistance coefficient ζ (zeta) is calculated by means of a dimensionless criterial equation:

$$\zeta = (1/\varphi^2 - 1) \cdot ((1 - \Omega)/\Omega)^{1.75}$$

where φ = 0.85–0.91 is the flow velocity coefficient; Ω is the perforation coefficient of the barrier. The energy loss resulting from the springboard effect at the foot of the cascade is determined using the modified Bernoulli equation:

$$\Delta E_{kin} = \zeta \cdot V_1^2/(2g) + (H_1 + p_1/\gamma_s) - (H_2 + p_2/\gamma_s)$$

The share of dissipated energy (the dissipation coefficient) is ultimately calculated as the efficiency criterion. According to the laboratory results presented in Section 3.1, even under the regime with the highest hydraulic load (Q = 0.250 m³/s, i = 0.06), the cascade structure dissipated up to 63.8% of the energy, which proves an efficiency 25-30% higher than that of conventional dams.

Model for reducing the level of damage. The relationship between the share of dissipated energy η and the expected damage in the lower basin is expressed by means of a linear-functional model. The level of residual risk (damage) after the installation of the structure:

$$R = R_0 \cdot (1 - \eta) \cdot k_t$$

where R_0 is the expected damage in the initial state (without the barrier); k_t is a correction coefficient taking into account the slope dynamics and the evacuation time. The relative reduction of the damage percentage:

$$\Delta U = (1 - R/R_0) \cdot 100\%$$

According to the field results, the structure reduces the channel slope from 15^0 to $4^0 \div 11^0$, thereby considerably decreasing the flow velocity. This creates the additional strategic time reserve (Δτ) required for moving the population of settlements and the citizens at recreational facilities in the lower part to a safe area, and it minimizes the damage percentage.

Unified iterative computational algorithm. By integrating the three blocks presented above, an iterative computational algorithm predicting the dynamic state of the frame-elastic barrier was developed. The algorithm consists of the following consecutive stages:

1. Input of the initial data: γ, w, V, φ, h_0, P%, i, F_1/F_0, t/T, Ω, as well as the frame geometry and the net opening size (0.20×0.20 m).

2. Hydrological block: calculation of the erosion coefficient E(t), of A(P%), and of the maximum discharge Q_{max}.

3. Hydrodynamic block: determination of the coefficients ψ, α, f(m) and of the specific impact pressure P_1.

4. Distribution along the height: construction of the parabolic profile P(z) and determination of P_{max} at the critical point $z^* = H_{1/3}$.

5. Verification of the strength condition: if $P_{max} > [P_{adm}]$, increase the frame cross-section or the anchor parameters and return to Stage 2.

6. Energy block: calculation of ζ, ΔE_{kin}, and of the dissipation coefficient η.

7. Verification of the efficiency condition: if $\eta < \eta_{min}$ (60%), change the number of cascades or the parameters Ω, φ and return to Stage 5.

8. Damage assessment: determination of the residual risk R, of the damage reduction ΔU, and of the evacuation time reserve Δτ.

9. Output of the results: Pmax, η, ΔU, Δτ, and the change of slope ($15^0 \rightarrow 4^0 \div 11^0$).

The logical sequence of this algorithm is fully reflected in the following block diagram (Figure 6).

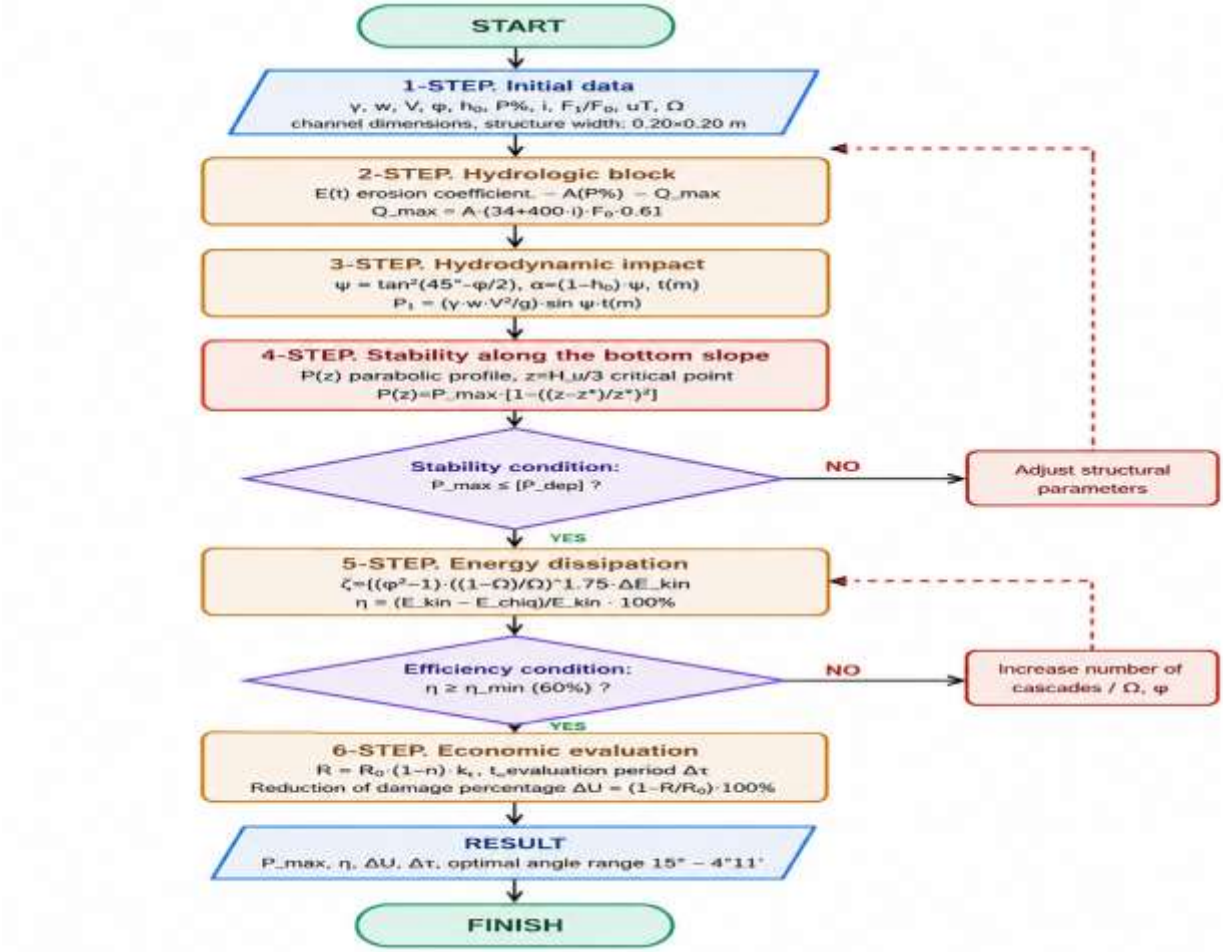

Figure 6. Block diagram of the algorithm for calculating the dynamic state of the frame-elastic barrier

The hydrological, hydrodynamic, and energy processes were generalized within a unified mathematical model. The developed iterative algorithm makes it possible to predict comprehensively the dynamic state of the frame-elastic barrier - the parabolic distribution of the impact pressure along the height, the degree of dissipation of the kinetic energy, and the reduction of damage in the lower basin.

The scientific novelty of the model lies in the fact that, unlike conventional rigid dams, it substantiates mathematically the mechanism of energy dissipation through elastic deformation and the location of the impact force at the critical point (the lower one third of the height). The iterative approach, which jointly verifies the strength ($P_{max} \leq P_{adm}$) and efficiency ($\eta \geq \eta_{min}$) conditions, provides a practical engineering tool for designing the structure with optimal parameters and for ensuring the safety of the population.

The monitoring results obtained during the first major debris-flow event at the structure installed in the Bostonliq district confirmed the laboratory predictions under real physical conditions. When the level of the rock material accumulated in the net reached 1.0 m, a boulder weighing 1.15 tonnes contained within the flow was successfully retained by the structure, and the total volume of the retained debris-mud mass amounted to 115 m³. As a result of the action of the structure, the channel slope decreased from 15^0 to $4^0 \div 11^0$, which ensured a considerable reduction of the flow velocity and of the subsequent impact force.

Table 3

Variation of the energy dissipation coefficient (η) under different hydraulic load regimes

Load regime	Q (m³/s)	i (channel slope)	η, %
Low	0.050	0.02	**41.2**
Medium	0.120	0.04	**52.6**
High	0.190	0.05	**58.9**
Maximum	0.250	0.06	**63.8**

The results obtained demonstrated the following practical advantages: (i) high kinetic resistance - the impact of large rock masses of up to 1.15 tonnes was safely withstood without brittle fracture; (ii) channel stability - the deep erosion of the riverbed was arrested; (iii) protection of the population - an additional strategic evacuation time reserve was created owing to the sharp reduction of the flow velocity. [13]

Distribution of the impact pressure along the height. The most important scientific result established through the analysis of the readings of the pressure sensors is that the impact pressure is distributed along the height (z) of the structure not uniformly, but according to a parabolic law. The critical point (z*) is located within the lower one third of the height of the structure ($z^* = H_{t/3}$), and the distribution was expressed by means of the following model (Figure 5):

$$P(z) = P_{max} \cdot [\, 1 - ((z - z^*) / z^*)^2 \,]$$

This result differs fundamentally from the assumption adopted for conventional rigid dams concerning the linear or hydrostatic distribution of pressure, and it experimentally confirms the load-redistribution property of elastic frame systems.

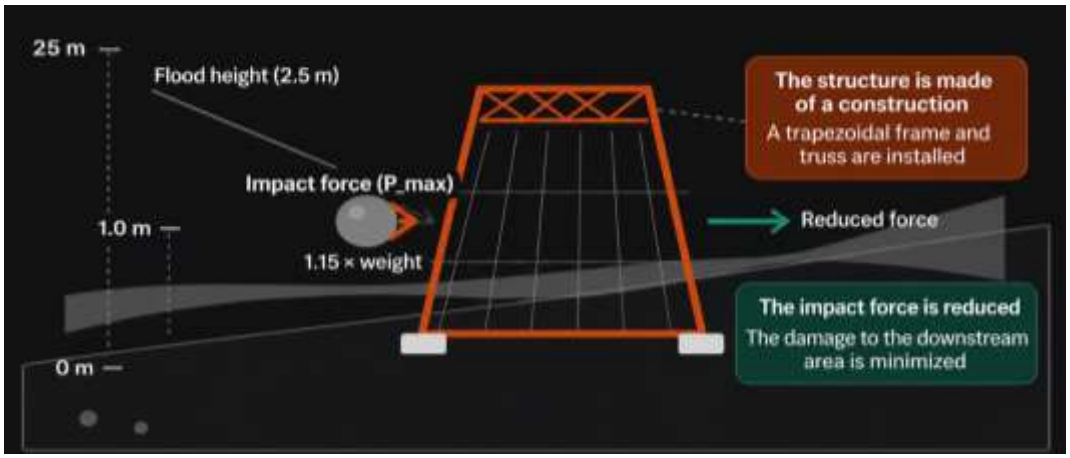

Figure 7. Mechanism of the dissipation of impact energy by the elastic metal structure

The results obtained reveal the fundamental difference between conventional rigid dams and the proposed frame-elastic barrier. Rigid structures operate mainly on the logic of "returning" the impact energy through reflection, which gives rise to a high concentration of stress in the body of the structure and, in the case of heavy loads, to the risk of brittle failure. The proposed elastic system, by contrast, is realized through a three-tier cascade and a two-stage decision mechanism based on the logic of "distributing" the energy throughout the entire volume of the structure by means of elastic deformation, which explains the high dissipation efficiency observed (63.8%).

The result concerning the parabolic distribution of the impact pressure and the location of the critical point within the lower one third of the height is of practical engineering importance: it requires that, in designing the structure, the anchors and supporting elements be reinforced in a manner directed precisely at the critical zone rather than distributed uniformly, which makes it possible to optimize material consumption and to reduce the cost of the structure. This result provides a more precise, localized design criterion in comparison with the generalized hydrostatic approaches recommended by G.V. Gavardashvili and B. McArdell for Alpine and Caucasian conditions.

The two-condition (strength and efficiency) structure of the iterative algorithm presented makes it possible to design the structure not only statically but also dynamically, with the possibility of recalculation for various hydrological scenarios. Furthermore, the mechanism of integration into the emergency management system, whereby the efficiency of the structure becomes a quantitative indicator measurable not only from a hydraulic-engineering but also from a resource-saving standpoint, constitutes a comprehensive approach that is rarely encountered in contemporary civil-protection research.

Conclusion. As a result of the conducted study, the hydrodynamic principles, the mathematical model, and the computational algorithm of a frame-elastic barrier structure that dissipates, through elastic deformation, the dynamic impact of debris-flow and flood currents in the mountainous and foothill regions of Uzbekistan under climate change conditions were developed and were scientifically validated under laboratory and real field conditions. The principal scientific results are summarized as follows:

1) The elastic structure dissipates up to 63.8% of the kinetic energy, thereby providing an efficiency 25-30% higher than that of conventional rigid dams;

2) The impact pressure is distributed along the height of the structure according to a parabolic law, and the critical point is located within the lower one third of the height;

3) A unified mathematical model integrating the hydrological, hydrodynamic, and energy blocks, together with an iterative algorithm jointly verifying the strength and efficiency conditions, was developed;

4) The developed approach serves as a scientifically grounded and practically tested engineering tool for managing the debris-flow and flood hazard in mountain watersheds under climate change conditions, and it constitutes a methodological basis that may be applied in other similar regions of the Republic of Uzbekistan.

References:

1. O‘zbekiston Respublikasi Prezidentining 2025-yil 20-oktyabrdagi “Aholi va hududlarni favqulodda vaziyatlardan ishonchli muhofaza qilish sohasini sifat jihatidan yangi bosqichga ko‘tarish to‘g‘risida” gi PF-185-son.
2. O‘zbekiston Respublikasi Prezidentining 2025-yil 20-oktyabrdagi “Favqulodda vaziyatlardan muhofaza qilish sohasini raqamlashtirish hamda ilmiy va innovatsion faoliyatni rivojlantirish chora-tadbirlari to‘g‘risida”gi PQ-311-son.
3. O‘zbekiston Respublikasi Prezidentining 2022-yil 28-yanvar kunidagi “2022-2026 yillarga mo‘ljallangan Yangi O‘zbekistonning taraqqiyot strategiyasi”ning “Mamlakatimiz xavfsizligi va mudofaa salohiyatini kuchaytirish, ochiq, pragmatik va faol tashqi siyosat olib borishning 92-maqsadi-Favqulodda vaziyatlarning oldini olish va bartaraf etishning samarali tizimini yaratish ustuvor yo‘nalishi hamda asosiy vazifalari to‘g‘risidagi PF-60-son.
4. O‘zbekiston Respublikasi Prezidentining 2022-yil 18-noyabrdagi “Xavfli gidrometeorologik hodisalar va geologik jarayonlar bilan bog‘liq favqulodda vaziyatlardan aholi va hududlarni muhofaza qilish chora-tadbirlari to‘g‘risida”gi PQ-426-son.
5. Shamansurov, S.S., Barotov M.B., Abduraximxo‘jayeva M.B. O‘zbekiston Respublikasi tog‘li hududlarida sel va suv toshqinlarining oldini olish va ularni samarali bartaraf etishning zmonaviy usullari. “Aniq va tabiiy fanlar yo‘nalishida ilmiy tadqiqotlarda favqulodda vaziyatlarning oldini olish va ularni samarali bartaraf etishning zamonaviy yechimlari” mavzusidagi ilmiy - amaliy anjuman. 2024-yil.
6. G.M.G‘ulomova, M.B.Barotov. Tabiiy xususiyatli favqulodda vaziyatlarda aholi xavfsizligini ta’minlash usullarini tahlili. “Ekologik xavfsizlik, mehnatni muhofaza qilish va favqulodda vaziyatlarni boshqarish integratsiyasi: inson va tabiatni himoya qilishga integrasiyalashgan yondashuv” xalqaro ilmiy-amaliy anjuman 2026 yil 29-30 aprel. SAMDAQU.
7. Gulomova, G.M., Shamansurov, S.S., Barotov M.B. O‘zbekiston Respublikasida tog‘li hududlarida iqlim o‘zgarishi natijasida sel va suv toshqinlarning tahlili. Inson kapitali va mehnatni muhofaza qilish ilmiy-amaliy electron jurnal. ISSN: 3060-49-82. №3(3)2024.
8. DEBRIS FLOWS: Disasters, Risk, Forecast, Protection. Proceedings of the 7th International Conference Chengdu, China, 23-27 September 2024
9. Gulomova G.M., Barotov M.B. *To the adsorbent obtained on the basis of local Angren coal analysis of adsorption energy properties of benzene vapors*. E3S Web of Conferences 461, 01071 (2023), 2023-yil.
10. Ermatova Y.S. Chorvoq botiqligining kurort zonalari geoekologik sharoitini saqlashda tabiiy va texnik tizimlar monitoringiga kompleks yondashuv. Geologiya - mineralogiya fanlari bo‘yicha falsafa doktori (PhD) ilmiy darajasini olish uchun yozilgan DISSERTATSIYA. Toshkent - 2025.

11. Brighenti R., Segalini A., and Ferrero A.M. Debris flow hazard mitigation: A simplified analytical model for the design of flexible barriers. Computers and Geotechnics, 54: 1-15. 2013.
12. Corinna Wendeler, Axel Volkwein, Brian W. McArdell, Perry Bartelt. Load model for designing flexible steel barriers for debris flow mitigation// Canadian Geotechnical Journal. August 2018 https://doi.org/10.1139/cgj-2016-0157
13. Xingyue Li, Jidong Zhao, Julian S.H. Kwan. Assessing debris flow impact on flexible ring net barrier: A coupled CFD-DEM study. Computers and Geotechnics Volume 128, December 2020. https://doi.org/10.1016/j.compgeo.2020.103850
14. Gulomova, G., Turabekova, U., Nizamova, D., Mudarisova, R. Problems of ensuring security in open – pipe coal mines in the republic of Uzbekistan. E3s Web of Conferences, *461, 01067,* 2023
15. Yong Kong, Xingyue Li, Jidong Zhao, Mingfu Guan. Load-deflection of flexible ring-net barrier in resisting debris flows. //Geotechnique//. Volume 74, Issue5, 25 October 2022, Pages 486-498. https://doi.org/10.1680/jgeot.22.00135
16. Axel Volkwein, Corinna wendeler, Guido Guasti. Design of flexible debris flow barriers. //Italian Journal of Engineering Geology and Environment – Book// Casa Editrice Università La Sapienza. 2011. *DOI:10.4408/IJEGE.2011-03.B-118.* www.ijege.uniroma1.it.
17. Aliena M. Debelak, Christopher A. Bareither, Hussam Mahmoud. Finite-Element Model of Impact Loading and Deformation of a Flexible Steel Ring-Net Debris-Flow Barrier. // Natural Hazards Review//**.** Jun 9, 2020. Vol. 21, №3**.** https://orcid.org/0000-0003-3427-4344.